DIVISION S-6—SOIL & WATER MANAGEMENT & CONSERVATION

Runoff Features for Interrill Erosion at Different Rainfall Intensities, Slope Lengths, and Gradients in an Agricultural Loessial Hillslope

Vincent A. M. Chaplot* and Yves Le Bissonnais

ABSTRACT

Various interactions, particularly those existing between the rainfall intensity, the slope gradient, the slope length, and the tillage supposedly can affect the runoff features for interrill erosion. Despite numerous studies, their effect on runoff production and pathways and the resulting soil losses have seldom been analyzed. This is especially true under field and tillage conditions. This study investigated the effect of rainfall intensity, slope length, and gradient on runoff amount and pathways for interrill erosion in tilled fields. Runoff features and soil losses were evaluated on bounded plots of 1- and 5-m length located on 4 to 8% slope gradients, and under natural and simulated rainfalls with intensities ranging from 1.5 to 30 mm h^{-1}. Runoff coefficients (R) ranged from 34 to 98% whereas sediment concentrations (SC) varied from 2.9 to 49 g l^{-1}. The runoff coefficient was affected by all three factors: rainfall intensity (r = 0.48; P < 0.0001), slope gradient (r = 0.51; P < 0.0001) and slope length (r = 0.29; P = 0.02); whereas SC was correlated with only rainfall intensity (r = 0.48; P < 0.0001) and slope length (r = 0.44; P = 0.0004). The runoff coefficient and SC ratios between 1- and 5-m long plots were systematically greater for the intermediate rainfall intensity. Runoff features mainly affected by tillage implements may explain higher interrill erosion at longer and steeper slopes. Lower differences between 1- and 5-m plots at high rainfall intensity may reflect greater ponded runoff absorbing raindrop kinetic energy and lowering detachment and transport processes. Finally, the effects of rainfall intensity, slope length, and gradient and tillage are discussed in respect of possible erosion processes operating in the experiments.

Water movement within landscapes is fundamental for the prediction of soil erosion and the conservation of water (Mermut et al., 1997). Rainwater not only moves up and down through the soil profiles and saprolites by percolation and evaporation, but also moves laterally on the surface and through the subsurface. Redistribution of soil particles by surface flow remains the most important factor in tropical and intertropical areas because of extreme rain events (e.g., Puigdefabregas et al., 1999). In temperate climates, overland flow predominates when the natural infiltration capacity of the soil surface is altered (Valentin and Bresson, 1992).

Soil loss rate (SL, mass per surface and time unit) may be defined as:

$$\mathrm{SL} = V \times \mathrm{SC} \qquad [1]$$

With V, the volume of surface water per time unit and SC, the mass of sediment per unit volume of water.

In agricultural landscapes, factors affecting V under steady-state conditions of infiltration are well documented (Kinnell, 2000). The effect of slope angle on runoff for interrill erosion has also been fully investigated. Runoff may increase at steeper slopes because of a decrease of the ponds' ability to retain water (Fox et al., 1997). Several authors have confirmed the influence of slope gradient on soil losses by interrill erosion (Huang, 1995; Fox and Bryan, 1999). The increase of detachment and transport of soil particles with higher flow velocity has already been demonstrated by laboratory experiments (Torri and Poesen, 1992; Fox and Bryan, 1999) and field investigations (e.g., Chaplot and Le Bissonnais, 2000). Fox and Bryan (1999) argued: "For a constant runoff rate rain impacted flow erosion increased roughly with the square root of the slope gradient (2 to 40%). Soil losses were correlated (r^2 = 0.81) with runoff velocity." However, Govers (1990) showed that slope gradient might have a significant negative effect on runoff and erosion because of differential soil cracking. Moss and Green (1983) attributed a decrease of interrill erosion at the steepest slopes to an increase in the water depth in ponds. When this depth exceeds the diameter of two drops it protects the soil surface from drop impact (Kinnell and Cummings, 1993). It is also well known that R and SC increase with the increase of rainfall intensity (e.g., Wischmeier and Smith, 1978; Fraser et al., 1999) because of: (i) the augmentation of runoff fraction of rainfall (Williams et al., 2000); (ii) the augmentation of soil detachment with increasing drop detachment forces (Kinnell, 1990; Torri and Poesen, 1992; Mermut et al., 1997) and (iii) a better transport and remobilization of particles by rain-impacted flow (Hairsine and Rose, 1992; Chaplot and Le Bissonnais, 2000). However, in some conditions, especially when a crust surface was formed quickly, no significant relation has been found between soil loss and rainfall parameters from 10 to 103 mm h^{-1} (Uson and Ramos, 2001).

Limited studies have been conducted to investigate the effect of slope length on runoff for interrill erosion, especially under field conditions. Since overland flow velocity is important for soil detachment and transport capacity, the interrill erosion rate should also be strongly influenced because longer slope lengths allow higher runoff velocities. Using field surveys Horton (1945) was one of the first to quantify the effects of the slope steepness and length. He demonstrated that erosion increases

V.A.M. Chaplot, IRD- Ambassade de France, BP 06. VIENTIANE, LAOS PDR. Y. Le Bissonnais, INRA, Science du Sol, Avenue De lab Pomme de Pin, B.P. 20619, Ardon, 45166 Olivet cedex, France. Received 28 June 2001. *Corresponding author (chaplotird@laopdr.com).

Published in Soil Sci. Soc. Am. J. 67:844–851 (2003).

Abbreviations: CEC, cation-exchange capacity; DEM, digital elevation model; SC, sediment concentration; SL, soil loss rate.

on longer and steeper slopes because of the increase of shearing forces on the soil surface. Such a relationship between slope length and soil losses was further used as a basis for the length slope (LS) factor of the USLE (Wischmeier and Smith, 1978) and more recently, Kinnell (2001ab) in the USLE-M.

Although considerable progress in establishing a more accurate relationship between runoff features for interrill erosion and biophysical factors has been made, the physical basis for this relationship remains largely unaccounted for. This may partly explain the lack of accuracy of currently used prediction models of erosion models (Boardman and Favis-Mortlock, 1998; Jetten et al., 1999). According to these authors, another reason for this could be the existence of strong interactions between erosion factors that are not well identified and are even less taken into account during modeling procedures. For instance, Meyer and Harmon (1989) showed that the effect of the slope length and steepness on erosion from interrill areas depended on rainfall intensity. Studies conducted by both Kinnell and Kummings (1993) and Huang (1995) have indicated the importance of soil properties in defining the relationship between slope steepness and soil loss on short slopes. More recently, Gabriels (1999) in the comparison of rainfall intensities (22.0 and 78.5 mm h^{-1}) applied on a sandy loam and a loamy sand from short slopes (between 0.3 and 0.9 m) stated that the slope length effect was soil dependant: "For the loamy sand the slope length effect was less for the large aggregate sizes which contained more sand than the original soil." Yet another explanation of the lack of accuracy of prediction models could be the failure to take into account the spatial variability of runoff features that may be controlled by environmental factors such as topography and agricultural practices (Souchère et al., 1998; Planchon et al., 2000; Takken et al., 2001).

Despite numerous investigations, quantitative data are not available to better understand the interactions between slope angle and length, and rainfall intensity on runoff amount and pathways for interrill erosion. Attempts are now in progress to consider these interactions in models such as the Water Erosion Prediction Project (WEPP) (Nearing et al., 1989), the Raindrop Induced Flow Transport model (RIFT) (Kinnell, 1988, 1991), the stream power based model (Hairsine and Rose, 1992), the EUROSEM (Morgan et al., 1998), and the USLE-M (Kinnell, 2001ab).

In Northern Europe, surface sealing and roughness, either natural or induced by tillage in agricultural areas, have large impacts on soil surface infiltration, runoff patterns, and consequently erosion (Le Bissonnais et al., 1998; Martin, 2000). In this study, our aim was to investigate the effect of rainfall intensity, slope length and gradient, and tillage on runoff features for interrill erosion under loamy soil conditions. We studied, in the field, experimental plots under natural and simulated rainfalls. Samples were collected for runoff, sediment concentration and soil loss evaluations. Additional measurements of water ponded and flow pathways were performed.

MATERIALS AND METHODS

Site Description

The study was conducted in northwestern France (Pays de Caux) in an experimental parcel of 1 ha, which encompassed the lower part of a 500-m long convex hillslope with an elevation of 15 m. The study parcel was part of a 100-ha basin supporting cereals, legumes, and pastures. The soil cover, developed into a silty loamy material from eolian origin overlying limestone, is predisposed to soil crusting because of its low clay and organic matter content (Le Bissonnais et al., 1998). Soils (Kandiudalfs) that did not significantly vary along the study hillslope were characterized (0- to 10-cm depth) by a clay content of 130 g kg^{-1}, a low organic C content (108 g kg^{-1}) and a low cation-exchange capacity (CEC) (10.5 $cmol_c$ kg^{-1}). The soil is mainly composed of coarse silts and fine sands (425 and 280 g kg^{-1}, respectively). In the region studied, rainfall intensities are generally moderate with low cumulate volumes in winter and at the beginning of spring. The periodicity of a rainfall with a 20-mm amount and 10-mm h^{-1} intensity is 3 yr (Le Bissonnais et al., 1998). The topography is gentle with slope angles varying from 8% on downslope position, 4% on upslope to 1% on summit. Three 1 by 1 m^2 and three 2 by 5 m^2 plots were established at upslope and downslope positions. The plots were bounded by metal borders inserted to a depth of 0.1 m.

Topographic Analysis of the Experimental Plots

A detailed topographical investigation was performed across the studied hillslope. One benchmark with a horizontal accuracy of better than 1-m was obtained using a differential Global Positioning System (GPS). From this mark, an infrared laser theodolite was utilized to register *x*, *y*, and *z* coordinates of complementary points. For the 1-m length plots, 36 measurements were performed within each plot according to a 0.2-m grid mesh. Additional 32 data according to a 1-m grid mesh were collected in its vicinity, in an area of 24 m^2 surrounding each plot. The same procedure was performed for the 5-m length plots except that the surrounding area had a 44-m^2 surface area. Afterwards, fine 0.2-m digital elevation models (DEMs) were constructed for each experimental plots including the surrounding area using the grid function of Arc Info 7.1 ESRI (1997). Mean slope gradients were estimated for each plot using the grid function of Arc Info 7.1 ESRI (1997). To evaluate the surface roughness of each plot, we calculated the standard deviation of altitudes normalized by the mean altitudes of points situated on the same perpendicular to the steepest slope.

Soil Surface Conditions

Plots were tilled along the direction of steepest slopes and sowed with winter wheat in late September 1994. Measurements were performed from January to March 1995 under a vegetation cover of about 10% and a well-developed surface crust that had received 450 mm of rain since sowing. The surface crust had formed as a result of the low aggregate stability of the silty material and because of continuous low intensity rainfall. We considered that measurements were performed under conditions of steady-state interrill erosion because surface microtopography and crust morphology did not vary during the study period. In addition, no significant soil cracking and rills were observed.

Runoff and Erosion Measurements

During the study period, six natural rainfall events were considered between 2 Feb. to 9 Mar. 1995. In addition, 30 mm

h^{-1} rainfall simulations were applied between 9th and 14th of March on the 1- and 5-m plots using an ORSTOM simulator (Valentin, 1978). The simulator was constituted by an oscillating nozzle (Teejet SS 6560) located 3.5-m above the plots. A valve and a pressure gauge were located at the same altitude of the nozzle allowing a precise control of water pressure and consequently the constancy of rain kinetic energy. At a water pressure of 40 kPa the estimated kinetic energy was 25 J m^{-2} mm^{-1}. For each plot, an initial 15 mm of rainfall was applied at the rate of 30 mm h^{-1} for 30 min before measurements to obtain steady-state conditions of runoff and erosion. Afterwards, runoff and sediment concentration samples were collected under the same rainfall conditions during three episodes of 30 min. Before each rain event, rainfall intensity and its spatial variations were determined to be <5% by using small bowls placed at each node of a 0.2- and 1-m grid within the 1- and 5-m length plots, respectively.

After each natural rainfall, the total runoff of each plot repetition was measured and an aliquot sample was collected. Afterwards, samples were dried and weighed to estimate their sediment concentration. For simulated rainfalls, runoff volume measurements and sample collection were performed each minute. The collected samples were also dried and weighed to evaluate SC and SL. Because of the accidental destruction of one 5-m length plot, only samples of the two remaining plot repetitions were considered. Finally, a total of 780 samples were collected for both natural and simulated rainstorms.

Spatial Distribution of the Ponded Water, Its Depth, and Water Pathways

Evaluations of depth of ponded water and spatial distribution of flow pathways are generally performed under laboratory conditions using quantitative methods. These methods consist of taking precise height measurements over a surface to construct DEMs. Laser roughness meters are useful tools for generating high precision DEMs (e.g., Kamphorst and Duval, 2001). The storage capacity of ponds and runoff pathways can be estimated by virtually filling the DEMs. However, under natural conditions, such estimations may differ from natural situations because of infiltration through the soil surface (Kamphorst and Duval, 2001). In our study, measurements of depth of ponded water were empirically performed using a rod and ruler system with a vertical resolution of ± 0.5 mm. In each 5-m plot, ponded-water depth was evaluated at 122 points on a 0.2 by 0.5 m grid. Each cell was wider in the up and down slope direction. Ponded depth maps were generated by ordinary kriging, a common interpolation method thoroughly described in the literature (e.g., Burgess et al., 1981). The predicted ponded depth at an unknown point used the observed depth values from the neighboring sample points and combined them linearly with weights derived from the inference of the experimental variogram. The experimental variogram or isotropic variogram of ponded depth was calculated and inferred from the whole data set. Directional variograms (0°, parallel to the contour lines; 45°; 90°, up and down slope; and 135°) were also generated from this set. Ponded-depth maps were afterwards generated on a 0.05 by 0.05 m grid from the best-fitted model of the isotropic variogram by using the GSLIB software (Deutsch and Journel, 1992).

Additional measurements were performed to evaluate the spatial organization of runoff pathways. Flow velocity measurements were performed using the data of Chaplot and Le Bissonnais (2000). A salt solution (45 g L^{-1} NaCl) colored with Fluorescein (3′,6′-Dihydroxyspiro[isobenzofuran-1(3H), 9′-[9H]xanthen]-3-one) was injected at various positions within the 5-m length plots. Flow velocity, V was calculated by dividing d, the distance between the injection and outlet points by the time difference between the injection of saline solution T_o, and the peak in electrical conductivity T_f:

$$V = \frac{d}{T_f - T_o} \quad [2]$$

The electrical conductivity of the runoff was monitored at the outlet of the plots after each salt solution injection. The peak in electrical conductivity corresponded to average flow velocity.

A limited data set of 10 to 15 locations, depending on within-plot variability (Chaplot and Le Bissonnais, 2000), was used for flow velocity evaluation. The spatial distributions of flow pathways and velocity within plots were visually interpolated.

Statistical Analysis

Variance analysis was performed on the data set. Under the null hypothesis, that there are no mean differences between groups in the population, the variance estimated from the within-group variability should be about the same as the variance estimated from between-groups variability. Statistical significances of results were evaluated using the p level, considering values that yield 0.05 (*) and 0.01 (***) as statistically significant and highly significant, respectively. To complement this, the interrelations between runoff and sediment production from interrill erosion and investigated variables (rainfall intensity and topographic parameters) were modeled using classical forward stepwise multiple regressions (Neter et al., 1989). The independent variables rainfall intensity, slope gradient, and length are easily accessible. Using these independent variables, multiple regressions allow the prediction of the dependent variables R, SC, and SL, difficult to access. When deciding whether a dependent variable would be added or removed during each step in the stepwise technique, a level of significance of 0.01 was assigned based on a F-test statistic (Neter et al., 1989).

RESULTS

Rainfall Characteristics

There occurred six natural rain events characterized by a total amount of about 100 mm. The maximum rainfall intensity (8 mm h^{-1}) and amount (16 mm) were observed on 16 through 17 Feb. 1995. The other five events showed mean intensities ranging from 1.3 to 1.7 mm h^{-1} and rainfall amount ranging from 2 to 46 mm: 2 Feb. 1995, 1.45 mm h^{-1}, 2 mm; 16 Feb. 1995 (collected at noon) 1.44 mm h^{-1}, 46 mm; 16 Feb. 1995 (collected at 2300 h) 1.55 mm h^{-1}, 5 mm; 8 Mar. 1995, 1.67 mm h^{-1}, 14 mm; 9 Mar. 1995, 1.31 mm h^{-1}, 5.4 mm.

Topographical Characteristics of the Study Plots

The mean slope gradient of the 1- and 5-m plots was 7.8% downslope and 4.1% upslope (Table 1). The

Table 1. Mean, Mean slope of plots; SD, Standard deviation of mean slopes (%); SD, Mean standard deviation of normalized altitudes (cm) according to the position on the hillslope and the slope length.

		Position in the hillslope		Slope length m	
		Downslope	Upslope	1	5
Slope gradient, %	Mean	7.82	4.10		
	SD	1.04	0.81		
Altitude, m	SD	2.02	1.98	2.22	1.80

standard deviation for slope gradients was in both situations close to 1% (1.0 and 0.8%, for 4 and 8% plots, respectively). Mean standard deviation of normalized altitudes (SD) differed slightly with slope positions and plot length. Values ranged from 1.98 cm downslope to 2.02 cm upslope, and from 1.80 cm for 5-m length plots to 2.22 cm for 1-m length plots, respectively.

The Effect of Rainfall, Slope Gradient, and Length on Runoff Amount

Runoff rates for plots of 1- and 5-m length under natural (1.5 and 8 mm h^{-1}) and simulated rainfall (30 mm h^{-1}) with slope gradients from 4 to 8% are shown in Table 2. Runoff coefficients are expressed as a percentage of the rainfall. The runoff coefficients ranged from 33.7 to 98%. An analysis of variance showed that runoff amount was significantly correlated to the rainfall intensity ($r = 0.48$; $P < 0.0001$), the slope gradient ($r = 0.51$; $P < 0.0001$) and the slope length ($r = 0.29$; $P = 0.02$) (Table 3).

Runoff increased with increasing rainfall intensity from, for instance, 33.7% at 1.5 mm h^{-1} to 57.0% at 30 mm h^{-1} from 1-m plots and on 4% slope gradient (Table 2).

From plots of 1 and 5 m, runoff was consistently greater from 8% than from 4% plots; the differences being more marked at high intensities: 33.7% versus 38.7% at 1.5 mm h^{-1}; 57% versus 89% at 30 mm h^{-1} on 1-m plots.

Runoff rate increased with plot length independently of the rainfall and the slope gradient. But on 5-m plots, it was greatest for the intermediate rainfall intensity. The runoff coefficient was from 1.0 to 1.8 times higher on 5-m plots than on 1-m plots, higher values being observed for intermediate rainfall intensity. Standard deviations between the three plot repetitions per treatment ranged from 1.8% for $R = 38.7\%$ on 1-m plot to 10.4% for $R = 72.7\%$ on 1-m plots.

The effect of rainfall intensity, slope gradient, and length on sediment concentration.

Sediment concentrations in runoff varied from 2.95 to 49 g L^{-1} (Table 2). Sediment concentration was significantly affected by rainfall intensity ($r = 0.48$; $P < 0.0001$) and slope length ($r = 0.44$; $P < 0.0001$). But only on 5-m plots was the effect of the slope gradient significant ($r = 0.51$; $P = 0.02$). Sediment concentrations increased with rainfall intensity (from 1.5–30 mm h^{-1}) but the highest SC occurred at an intermediate intensity. On 1-m plots and at a 4% slope gradient, SC increased from 2.95 g L^{-1} at 1.5 mm h^{-1} to 8.57 g L^{-1} at 8 mm h^{-1} but then decreased to 3.5 g L^{-1} at 30 mm h^{-1} (Table 2).

Sediment concentration was from 1.1 to 6.9 higher on 5-m plots than on 1-m ones. Minimum ratio values of 1.1 and 1.4 were encountered on 4% slopes and under the 1.5 and 30 mm h^{-1} rainfall conditions, respectively. Maximum SC was observed on 8% slopes and at the 8 mm h^{-1} rainfall. Finally, on 5-m plots, SC increased with slope gradient (from 4 to 8%) at a rate that was more acute for the 8 mm h^{-1} rainfall. Standard deviation between similarly treated plots for SC ranged from

Table 2. Mean, standard deviation (SD) between repetitions for runoff, sediment concentration and soil losses for the natural and simulated rainfall for 1- to 5-m long plots with slope gradients from 4 to 8%. Mean length ratio between the plots.

		Rainfall intensity, mm h^{-1}					
		1.5		8		30	
		Slope angle, %					
Slope length		4	8	4	8	4	8
m		Runoff, %					
1	Mean	33.7	38.7	51.7	72.7	57.0	89.0
	SD	2.9	1.8	9.6	10.4	5.2	6.7
5	Mean	60.3	63.3	94.0	98.0	60.0	92.0
	SD	5.1	9.6	6.5	10.1	7.1	3.5
5:1 ratio	Mean	1.8	1.6	1.8	1.3	1.1	1.0
		Sediment concentration, g L^{-1}					
1	Mean	2.9	3.2	8.6	7.1	3.5	3.6
	SD	0.8	0.1	2.3	0.3	1.1	0.7
5	Mean	4.1	11.2	15.8	49.0	4.0	7.0
	SD	0.9	4.4	3.5	10.2	0.9	1.0
5:1 ratio	Mean	1.4	3.5	1.8	6.9	1.1	1.9
		Soil Losses, g m^{-2} h^{-1}					
1	Mean	1.5	1.9	35.4	41.4	59.9	96.1
	SD	0.1	0.1	1.8	0.3	1.7	1.5
5	Mean	3.7	10.6	118.8	384.2	72.0	193.2
	SD	0.1	0.6	1.8	8.2	1.9	1.1
5:1 ratio	Mean	2.5	5.7	3.4	9.3	1.2	2.0

Table 3. Analysis of variance between runoff (*R*), sediment concentration (SC) and soil losses (SL) as independent variables and slope length (*L*), slope gradient (*G*) and, rainfall intensity (*I*) as dependent variables. Coefficient of correlation, *r*; mean square, MS; *F*-value and resulting *P* level used as an overall F test.

		r	df	MS	F	P level
All plots						
R	*I*	0.48	1	92.29	18.55	***
	G	0.51	1	66.89	21.79	***
	L	0.29	1	11.22	5.55	*
Regression equation: $R = 6.25 + 3.4 \times L + 4.9 \times G + 3.9 \times I$						
		0.56	3	13 945	25.29	***
SC	*I*	0.48	1	90.41	17.57	***
	G	0.18	1	8.36	1.96	NS†
	L	0.44	1	26.21	14.38	***
Regression equation: $SC = -1.31 + 2.0 \times L + 1.2 \times I$						
		0.55	2	1 152.22	25.86	***
SL	*I*	0.89	1	313.64	233.45	***
	G	0.23	1	14.71	3.64	NS
	L	0.43	1	25.73	14.60	***
Regression equation: $SL = -3.15 + 1.9 \times L + 1.2 \times I$						
		0.91	2	2 148.28	360.77	***
1-m plots						
R	*I*	0.65	1	7 992.41	51.72	***
	G	0.63	1	83.58	33.30	***
SC	*I*	0.75	1	179.48	64.70	***
	G	0.01	1	0.04	0.01	NS
SL	*I*	0.85	1	230.84	136.97	***
	G	0.17	1	6.79	1.64	NS
5-m plots						
R	*I*	0.71	1	39.13	17.0	***
	G	0.01	1	0.01	0.00	*
SC	*I*	0.76	1	44.68	10.63	*
	G	0.51	1	9.69	3.61	*
SL	*I*	0.85	1	1.00	56.72	***
	G	0.26	1	2.32	0.51	*

* Significant at the 0.05 probability level.
*** Significant at the 0.001 probability level.
† Not significant.

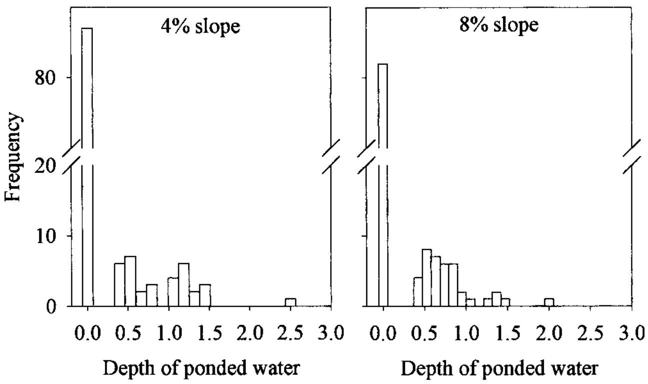

Fig. 1. Histograms of depth of ponded water (cm) for 5-m long plots at 4 and 8% slope angles.

0.11 g L^{-1} (when SC was 3.2 g L^{-1}) to 10.2 g L^{-1} (when SC reached 49 g L^{-1}) (Table 2).

The Effect of Rainfall Intensity, Slope Gradient, and Length on Soil Losses

Soil loss rates calculated as the product of sediment concentration and runoff time for a surface unit area and for 1 h of rain and are presented in Table 3. Soil loss rates ranged between 1.5 to $384 \text{ g m}^{-2} \text{ h}^{-1}$. Looking at both slope lengths, soil losses were significantly correlated to the rainfall intensity ($r = 0.89$; $P < 0.001$) and the slope length ($r = 0.43$; $P < 0.001$). As with SC, a significant correlation with slope angle was found for 5-m plots only ($r = 0.26$; $P < 0.05$). For 1-m plots, SL significantly increased with increasing rainfall intensity and slope gradient. For 5-m plots, highest SL occurred at the intermediate rainfall intensity (Table 2).

Spatial Distribution of the Depth of Ponded Water and Runoff Pathways

Histograms of depth of ponded water for 5-m plots on 4 and 8% slopes are presented in Fig. 1. On 4% plots, 87% of observations did not show any ponded water. In remaining 13%, depths of ponded water exhibited a bimodal distribution. Approximately 55% of these

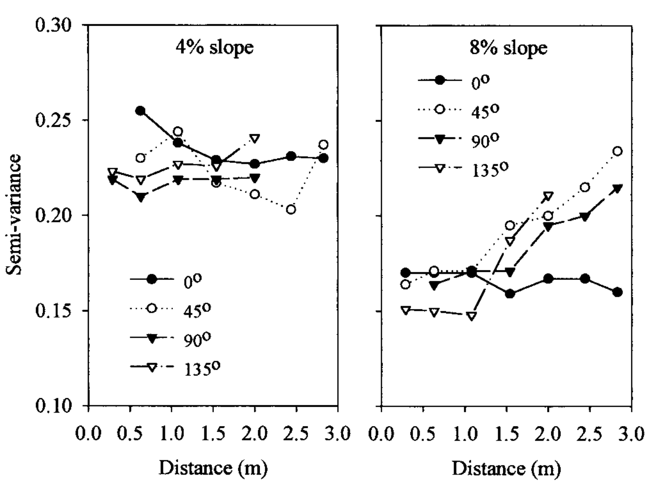

Fig. 2. Directional variograms (0°, parallel to the contour lines; 45°; 90°, up and down slope and; 135°) of the depth of water ponded for experimental plots of 5-m length on 4 and 8% slope gradient positions during a 30-mm h^{-1} artificial storm.

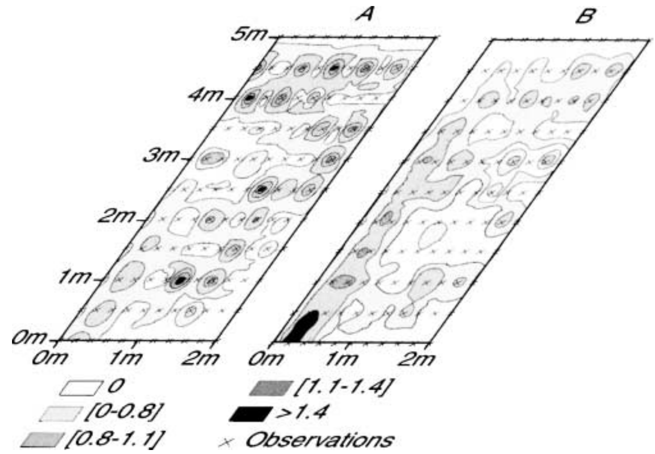

Fig. 3. Maps of the depth of water ponded performed by ordinary kriging using a data set a the nodes of an 0.2 by 0.5 m grid from a single experimental plot of 5-m length on 4 and 8% slope gradient positions during a 30-mm h^{-1} artificial storm and under steady-state conditions of runoff.

values were between 0.4 and 0.8 cm whereas 43% occurred between 1.0 and 1.5 cm. On 8% plots, the proportion of observations without ponded water reached 82%. Depths of remaining observations showed a unimodal and skewed distribution with a maximum frequency at 0.6 cm.

The spatial structure of water ponded depth on 4% plots is shown in Fig. 2A. Directional variograms showed high variability at short distances (<0.2 m). With increasing distance between observation points, the semivariance did not vary. This evidenced the absence of spatial dependency of data. The isotropic variogram was best fitted by a linear model (nugget = 0.23, slope = 0.0125). Directional variograms of ponding water depth under the 8% slope condition are presented in Fig. 2B. The semivariances were much lower than for the 4% plots. In addition, an anisotropy in two perpendicular directions could be observed. As for the 4% plots, the 0° direction (perpendicular to the steeper slope) and the 135° one generated a very slightly increasing variogram. In contrast, the 90° direction (parallel to the steepest slope) and the 45° direction displayed a high increase of semi variance with increasing distance.

The kriged maps of the water-ponded depth per slope position are presented in Fig. 3. For both maps, ponds showed a diameter less than two grid cells (40 cm). On the 4% position, pools did not seem to be connected except in the southwestern part of the plot where their water depths were lower than 1.1 cm and where flow velocity exceeded 5 cm s^{-1}. On the 8% plot, depths of ponded water of >0.8 cm were observed at the bottom, parallel to the steepest slope. These higher depths corresponded to areas of flow accumulation and concentration along preferential pathways with velocities between 5 and 25 cm s^{-1}. The remaining areas showed water ponded depths of between 0 and 1.1 cm.

DISCUSSION

Effect of Rainfall Intensity, Slope Gradient, and Length on Runoff Features

During the conditions of the study, the runoff (R), evaluated on bounded plots of 1- and 5-m lengths increased significantly with increasing rainfall intensity (up to 30 mm h^{-1}), slope angle (from 4 to 8%), and slope length (Eq. [3]).

$$R = f(I,G,L) \quad [3]$$

The increase of R with increasing rainfall intensity was concordant with previous observations of Wischmeier and Smith (1978); Fraser et al. (1999); Williams et al. (2000). This may be easily explained by the low level of infiltration of the crusted surface and its relative stability for whatever storm event. However, in this study longer plots exhibited a higher runoff for 8 mm h^{-1} intensity than for the 30 mm h^{-1}. An initial increase from 1.5 to 8 mm h^{-1} and a subsequent decrease to 30 mm h^{-1} was observed. This may be explained by increased depths of ponded water at high rainfall intensity inundating the structural crust and leading to an increase of infiltration rates as already observed by Fox et al. (1998) in laboratory experiments.

Runoff amount was also shown to increase with increasing slope angle. Such a result confirms previous observations of Huang (1995) and more recently Fox et al. (1997). According to these authors, an increase in R may be because of the lessening of the ponds' ability to retain water at steeper slopes. Any reduction in soil surface infiltration may result from interplay of one or more of the factors: decrease of overland flow depth, surface storage, and inundated surface.

Runoff was consistently higher for 5-m length plots than for 1-m ones. Variation of surface sealing between plot sizes may be involved. Indeed, in agricultural landscapes, surface sealing and its spatial variations may have large impacts on soil surface infiltration and runoff production. Generally sedimentary crusts with lower hydraulic conductivity (Valentin and Bresson, 1992; Desmet and Goovers, 1997) are found in depressions and microdepressions. Structural crusts are associated with soil mounds (Fox and Bryan, 1999). But in some cases, sedimentary crusts may mainly form in the downstream direction of plots because of increasing sedimentation possibilities when RIFT, the dominant transport system (Kinnell, 1990, 1991), becomes less efficient. This was observed in our experiment. Tillage-induced pathways may also cause differences between plot lengths. Plots of 1 m long showed bounded depressions with a mean diameter of ± 0.4 m that corresponded to the tillage and the planting implements. In addition, 5-m plots exhibited a single linear pathway in the direction of the steepest slope, which also corresponded to one wheel track of the tractor used during sowing. The second wheel track of the tractor was localized at a 3-m distance from this first one but outside the bounded plots. Wheel tracks that cause lower topographic variability and higher compaction may induce lower ponded storage and infiltration explaining more runoff. This confirms the sharp relation between tillage and runoff pathways as already shown by Ludwig et al. (1995), Souchère et al. (1998), Planchon et al. (2000), and Takken et al. (2001) on larger surfaces. In addition to this, these results may allow a better understanding of the effect of tillage-induced pathways on runoff amount.

The increase of runoff with increasing slope length was greater on 8% than on 4% slopes. This may be explained by lower depression storage capacities and higher depression connectivity on the steepest slopes. However, for the 30 mm h^{-1} storm, runoff did not increase with increasing slope length probably because of the combination of two mechanisms occurring at large rainfall intensities: (i) a reduced effect of surface depression on ponded storage at short lengths and; (ii) an increased infiltration rate downstream in longer plots because of the inundation by runoff of the structural crust leading to higher infiltration rates.

Consequences for Interrill Erosion

Sediment concentration was shown to be a function of rainfall intensity (I), slope length (L), and gradient (G) (Eq. [4]).

$$SC = f(I,G,L) \quad [4]$$

Chaplot and Le Bissonnais (2000) demonstrated that SC and SL increased with increasing slope angle and length. This leads to an increase in flow velocity which in turn results in better detachment, transport, and remobilization of particles by rain-impacted flow, this confirming in the field the validity of laboratory observations (Kinnell, 1990; Torri and Poesen, 1992; Mermut et al., 1997, Hairsine and Rose, 1992). Sediment concentration and soil losses (SL) were also significantly correlated to rainfall intensity, but this relationship does not appear to be simple. A quadratic behavior for SC and SL was observed: an initial increase between 1.5 and 8 mm h^{-1} and followed to a decrease to 30 mm h^{-1}. The decrease in SC and SL from plots as I increased from 8 to 30 mm h^{-1} may be explained by the removal from the soil surface of easily detachable particles (result of several mechanisms such as burrowing of insects, wetting, drying, or deposition during the recession of a previous hydrograph) during the initial 30 min rainfall before initiation of sampling.

Also surprisingly, medium rainfall intensity (8 mm h^{-1}) greatly enhanced slope gradient and slope length effects on SC and SL. On the contrary, high rainfall intensity (30 mm h^{-1}) induced only slight differences between slope gradients and lengths. This behavior cannot only be explained by the removal of easily detachable particles during the initial 30-min dry run. A possible explanation for this may be related to ponded runoff variations. Indeed, as I increases, so does R and ponded runoff. Greater ponded runoff may explain the lowering of soil losses by the interception of raindrop kinetic energy. Such effect of ponded runoff may also be associated with the effect of predetached particles on soil erodibility Kinnell (1990, 1991). Indeed, because RIFT is a detachment limited transport system, material being transported downstream should be stored as a layer of loose particles on the soil surface during the transport process (Kinnell, 2001ab). This has been observed within our study plots. The erodibility of the loose material is higher than of the underlying crusted surface, and the coverage layer of the lag material decreases as flow velocity increases, therefore the effective erodibility of the eroding surface tends to decrease with runoff rate.

This should explain lower erosion rates at higher rainfall intensities. Such dominance of any particular detachment and transport system in interrill erosion was shown here to change with slope gradient, length, and runoff conditions.

Finally, the current study suggested that the efficiency of detachment and transport was linked to runoff pathways affecting flow depth and velocity. The increase of erosion at longer and steeper slopes was related to higher connectivity between depressions caused by tillage practices (planting implements and wheel tracks) allowing higher runoff depth and velocity. With increasing runoff velocity the flow shear may reach such a level that detached particles falling back to the bed beneath the flow will immediately be entrained by the flow and then the erodibility of the surface would be much more controlled by detachment rather than by transport mechanisms. Rill erosion may also occur because of the flow shear. This was not observed in our experiment, that is, for slope length and gradients varying from 1 to 5 m and 4 to 8%, respectively and rainfall intensities between 1.5 and 30 mm h^{-1}.

CONCLUSION

In this study of an agricultural loessial hillslope, our main objective was to evaluate, under field conditions, the effect of the interactions between slope gradient, slope length, and rainfall intensity on runoff features and soil losses. This subject was investigated for different natural and artificial rainfall intensities (from 1.5–30 mm h^{-1}) on bounded plots differing in their slope gradient (4–8%) and their slope length (1–5 m). Results indicated an increase of runoff with rainfall intensity, slope gradient, and slope length but generally only rainfall intensity and slope length affected sediment concentration. Slope gradient had no impact on SC on 1-m plots but did on 5-m plots because of more sediment detachment and transport with increasing flow velocity. In addition, R, SC, and SL showed an initial increase from 1.5 to 8 mm h^{-1} followed by a decrease to 30 mm h^{-1}. This trend for runoff may be explained by the inundation of the structural crust by more intensive rainfall leading to higher infiltration rate. In addition, lower sediment concentration at high rainfall intensity may reflect greater ponded runoff absorbing raindrop kinetic energy and lowering RIFT effect on soil losses. Finally, this study quantified the relationship between interrill erosion and rainfall intensity, slope length, and steepness. The resulting better knowledge of processes involved under field conditions may improve soil erosion models.

ACKNOWLEDGMENTS

The authors are indebted to critical suggestions given by the two anonymous reviewers for their valuable comments and their improvement of the final manuscript. Special thanks go to Mr. B. Renaux from INRA Orleans for assistance with the field survey, and Maureen Brown for assistance in the final preparation.

REFERENCES

Boardman, J., and D. Favis-Mortlock. 1998. Boardman, J., and D. Favis-Mortlock, (ed.) Modeling Soil Erosion by Water. Springer, NATO-ASI Series I-55, Berlin, Germany.

Burgess, T.M., R. Webster, and A.B. McBratney. 1981. Optimal interpolation and isarithmetic mapping of soil properties. Sampling strategy. J. Soil Sci. 32:643–659.

Chaplot, V., and Y. Le Bissonnais. 2000. Field measurements of interrill erosion under different slopes and plot sizes. Earth Surf. Processes Landforms 25:145–153.

Desmet, P.J.J., and G. Govers. 1997. Two-dimensional modelling of the within-field variation in rill and gully geometry and location related to topography. Catena 29:283–306.

Deutsch, C.V., and A.G. Journel. 1992. Geostatistical sofware library and user's guide. Oxford Univ. Press, Oxford, U.K.

ESRI. 1997. Understanding GIS. The ARC/INFO method. ESRI, Redlands, CA.

Fox, D.M., R.B. Bryan, and A.G. Price. 1997. The influence of slope angle on final infiltration rate for interrill conditions. Geoderma 80:181–194.

Fox, D.M., Y. Le Bissonnais, and P. Quetin. 1998. The implications of spatial variability in surface seal hydraulic resistance for infiltration in a mound and depression microtopography. Catena 32:101–114.

Fox, D.M., and R.B. Bryan. 1999. The relationship of soil loss by interrill erosion to slope gradient. Catena 38:211–222.

Fraser, I., T.R., Harrod, and, P.M. Haygarth. 1999. The effect of rainfall intensity on soil erosion and particulate phosphorus transfer from arable soils. Water Sci. Technol. 39:41–45.

Gabriels, D. 1999. The effect of slope length on the amount and size distribution of eroded silt loam soils: Short slope laboratory experiments on interrill erosion. Geomorphology 28:169–172.

Govers, G. 1990. A field study on topographical and topsoil effects on runoff generation. Catena 18:91–111.

Hairsine, P.B., and C.W. Rose. 1992. Modelling water erosion due to overland flow using physical principles. 1. Sheet flow. Water Resour. Res. 28:237–243.

Horton, R.E. 1945. Erosional development of streams and their drainage basins: Hydrological approach to quantitative morphology. Geol. Soc. Am. Bull. 56:275–370.

Huang, C.-H. 1995. Empirical analysis of slope and runoff for sediment delivery from interrill areas. Soil Sci. Soc. Am. J. 59:982–990.

Jetten, V., A. de Roo, and D. Favis-Mortlock. 1999. Evaluation of field-scale and catchment-scale soil erosion models. Catena 37:521–541.

Kamphorst, E.C., and Y. Duval. 2001. Validation of a numerical method to quantify depression storage by direct measurements on moulded surfaces. Catena 43:1–14.

Kinnell, P.I.A. 1988. The influence of flow discharge sediment on sediment concentrations in raindrop induced flow transport. Aust. J. Soil Res. 26:575–582.

Kinnell, P.I.A. 1990. Modelling erosion by rain-impacted flow. Catena 17:55–66.

Kinnell, P.I.A. 1991. The effect of flow depth on sediment transport induced by raindrops impacting shallow flows. Trans. ASAE 34: 161–168.

Kinnell, P.I.A., and D. Cummings. 1993. Soil/slope gradient interactions in erosion by rain impacted flow. Trans. ASAE 36:381–387.

Kinnell, P.I.A. 2000. Effect of slope length on sediment concentrations associated with side-slope erosion. Soil Sci. Soc. Am. J. 64:1004–1008.

Kinnell. P.I.A. 2001a. Slope length factor for applying the USLE-M to erosion in grid cells. Soil Tillage Res. 58:11–17.

Kinnell, P.I.A. 2001b. Comments on"Vertical Hydraulic Gradient and Run-on Water and Sediment Effects on Erosion Processes and Sediment Regimes". Soil Sci. Soc. Am. J. 65:953–955.

Le Bissonnais, Y., H. Benkhadra, V. Chaplot, D. Fox, D. King, and J. Daroussin. 1998. Crusting, runoff and sheet erosion on silty loamy soils at scales and upscaling from m^2 to small catchments. Soil Tillage Res. 46:69–80.

Ludwig, B., J. Boiffin, J. Chadoeuf, and A.V. Auzet. 1995. Hydrological structure and erosion damage caused by concentrated flow in cultivated catchments. Catena 25:227–252.

Martin, F. 2000. Reducing food risk from sediment-laden agricultural runoff using intercrop management techniques in northern France. Soil Tillage Res. 52:233–245.

Mermut, A.R., S.H. Luk, M.J.M. Romkens, and J.W.A. Poesen. 1997. Soil loss by splash and wash during rainfall from two loess soil. Geoderma 75:203–214.

Meyer, L.D., and W.C. Harmon. 1989. How row sideslope length and steepness affect sideslope erosion. Trans. ASAE 32:639–644.

Morgan, R.P.C., J.N. Quinton, R.E. Smith, G. Govers, J. Poesen, K. Auerswald, G. Chisci, D. Torri, and M.E. Styczen. 1998. The European soil erosion model (EUROSEM): A dynamic approach for predicting transport from fields and small catchments. Earth Surf. Processes Landforms 23:527–544.

Moss, A.J., and P. Green. 1983. Movement of solids in air and water by rain drop impact. Effects of drop-size and water-depth variations. Aust. J. Soil Res. 21:257–269.

Nearing, M.A., G.R. Foster, L.J. Lane, and S.C. Finkner. 1989. A process-based soil erosion model for USDA-Water erosion Prediction Project Technology. Trans. ASAE 32:1587–1593.

Neter, J., W. Wasserman, and M.H. Kutner. 1989. Applied linear regression models. Richard D. Irwin.

Planchon, O., M. Esteves, N. Silvera, and J.M. Lapetite. 2000. Raindrop erosion of tillage induced microrelief: possible use of the diffusion equation. Soil Tillage Res. 56:131–144.

Puigdefabregas, J., A. Sole, L. Gutierrez, G. del Barrio, and M. Boer. 1999. Scales and processes of water and sediment redistribution in drylands: results from the Rambla Honda field site in Southeast Spain. Earth Sci. Rev. 48:39–70.

Souchère, V., D. King, J. Daroussin, and F. Papy. 1998. Effect of tillage on runoff directions: Consequences on runoff contributing area within agricultural catchments. J. Hydrol. (Amsterdam) 206: 256–267.

Takken, I., V. Jetten, G. Govers, J. Nachtergaele, and A. Steegen. 2001. The effect of tillage-induced roughness on runoff and erosion patterns. Geomorphology 37:1–14.

Torri, D., and J. Poesen. 1992. The effect of Soil Surface Slope on raindrop detachment in erosion, transport and depositional processes. Catena 19:561–577.

Uson, A., and M.C. Ramos. 2001. An improved rainfall erosivity index obtained from experimental interrill soil losses in soils with a Mediterranean climate. Catena 43:293–305.

Valentin, C. 1978. Problèmes méthodologiques liés à la simulation de pluies. Application à l'étude de l'érodibilité des sols. (In French.) Colloque "érosion agricole", Vogt, (ed.), Université de Strasbourg, 117–122.

Valentin, C., and L.M. Bresson. 1992. Morphology, genesis and classification of surface crusts in loamy and sandy soils. Geoderma 55: 225–245.

Williams, J.D., D.E. Wilkins, C.L. Douglas, J. Ronald, and W. Rickman. 2000. Mow-plow crop residue management infuence on soil erosion in north-central Oregon. Soil Tillage Res. 55:7–78.

Wischmeier, W.H., and D.D. Smith. 1978. Predicting rainfall erosion losses- A guide to conservation planning, USDA Agric, Handb. 537. U.S. Gov. Print. Office, Washington DC.